Cesium growth on the SrTiO 3 (100) surface Cesium growth on the SrTiO 3 (100) surface

Article *in* Materials Research Express · November 2015

DOI: 10.1088/2053-1591/2/11/116501

4 authors, including:

D. Vlachos
University of Ioannina
36 PUBLICATIONS **421** CITATIONS
SEE PROFILE

Matthew Kamaratos
University of Ioannina
81 PUBLICATIONS **1,019** CITATIONS
SEE PROFILE

Cesium growth on the $SrTiO_3$(100) surface

2015 Mater. Res. Express 2 116501

(http://iopscience.iop.org/2053-1591/2/11/116501)

Materials Research Express

PAPER

Cesium growth on the $SrTiO_3(100)$ surface

D Vlachos, E Giotopoulou, S D Foulias and M Kamaratos

Department of Physics, University of Ioannina, PO Box 1186, GR-451 10, Ioannina, Epirus, Greece

E-mail: dvlachos@cc.uoi.gr

Keywords: cesium, strontium titanate, adsorption

RECEIVED
11 August 2015

REVISED
24 September 2015

ACCEPTED FOR PUBLICATION
7 October 2015

PUBLISHED
3 November 2015

Abstract

We investigate Cs adsorption on the $SrTiO_3(100)$ surface at room temperature by means of Auger electron spectroscopy, low energy electron diffraction, electron energy loss spectroscopy, thermal desorption spectroscopy and work function measurements. Cesium grows in a single amorphous layer, showing different morphology from that on other insulating substrates. The Cs overlayer approximates a two-dimensional metallic phase. No indications for the reduction of the substrate and a Cs–O compound are found. Thermal annealing desorbs part of the metallic Cs, inducing at the same time the surface diffusion of the Cs adatoms to higher binding energy states. The growth and adsorption kinetics of Cs on the STO, shows substantial differences to that of other alkalis such as K and Li. The reasons for that are discussed.

1. Introduction

Metal-oxide (MO) interfaces have an extended range of usefulness in modern technology, based on their mechanical, chemical, electronic, optical and biocompatible properties. Thus, such interfaces find various applications in heterogeneous catalysis, contacts in microelectronic and photovoltaic devices, gas sensors, coatings for corrosion passivation, thermal barriers, oxide dispersion-strengthened alloys, metal/ceramic composites for medical implantation materials etc. The functionality of a MO interface depends on factors such as adhesion and mechanical strength, as well as chemical and thermal stability. Those factors are crucially determined by the structural and the electronic properties of the interface, which both are closely related to MO interactions [1–3]. Therefore, in order to define the properties of such a system, it is important to investigate from a microscopic point of view, possible interactions at the interface, consisting in either interfacial charge transfer (electronic interaction), and/or interfacial atom transport (chemical interaction) [3].

The preparation conditions and the characterization methods of the MO interfaces is a matter of a vast research effort so far, well described in several reviews [3–5]. Among metals, the alkalis are interesting adsorbates on oxide surfaces, since they are the simplest metals, are very reactive, usually reduce the work function (WF) of the substrate and enhance the oxidation process. On the other hand, oxide substrates such as the perovskite-type oxide strontium titanate $SrTiO_3$ (STO), show remarkable utility as a substrate for developing high-T_c superconductors [6], and as a buffer material for growing GaAs on silicon [7]. STO has also been used as oxygen gas sensor due to its electrical conductivity [8], as magnetic barrier in the magnetic tunnel junctions [9], and in the transistors industry due to its large electrostatic permittivity [10]. Moreover, a reduced $SrTiO_3(100)$ surface shows catalytic properties because of its reactivity toward decomposition of methanol [11] and water [12]. Regarding the latter, $SrTiO_3$ has been used as electrode in photoelectrochemical cells for electrolysis of water [13–15].

The alkali–STO interface is an intriguing adsorption system, since the electropositive alkali atoms tend to donate electrons, promoting the electron transfer at the interface. This may crucially alter the electronic and catalytic properties of the interface. So far only a few studies of alkalis adsorption on the STO(100) surface have been done. More particularly, Mori and Kamaratos have investigated Li [16] and K [17] adsorption at room temperature (RT). Lithium adatoms interact strongly with the surface probably through covalent bonding, intermix with the surface oxygen atoms and/or intercalate into the surface. Potassium adsorption, on the other

hand, shows a charge transfer from K 4 s to Ti 3d empty states, indicating an ionic bonding. For both alkalis, no chemical compounds with surface O atoms were detected. Moreover, neither Li or K forms a metallic state on the STO. Furthermore, sodium coadsorption with water on STO has been studied by means of high resolution electron energy loss spectroscopy (EELS) [18], suggesting a charge transfer process between Na 3s to Ti 3d states, thus turning Na adatoms into positive ions. More recently, Wang *et al* [19] studied also Na adsorption on the STO(100) surface using the density functional theory approach. The authors showed that Na adsorption is favorable on the TiO_2 surface termination rather than on the SrO one.

The present work aims to investigate the growth of cesium on the STO(100) surface at RT, by means of Auger electron spectroscopy (AES), low energy electron diffraction (LEED), EELS, thermal desorption spectroscopy (TDS) and measurements of the relative WF. Our purpose is to study the morphology of cesium growth as well as the stability of the interface from the kinetic, structural and chemical point of view. This is a preliminary work of our plan to study in detail the adsorption of water on the Cs/STO(100) interface, with a possible application to the dissociation of water for producing hydrogen gas.

2. Experimental part

The experimental process took place in an UHV chamber with the base pressure of the order of 10^{-10} mbar. The chamber was equipped with a four grid LEED optics, a Varian cylindrical mirror analyzer (CMA) with 0.3% energy resolution for AES and EELS measurements, a quadrupole mass spectrometer (QMS) for TDS measurements, and an electron gun for relative WF measurements by the diode mode.

The sample used as substrate was a single crystal of $SrTiO_3$(100) doped with Fe acceptors (0.14 wt%) purchased from crystal GmbH. The substrate was mounted on a *X*–*Y*–*Z* manipulator and fixed within a Ta foil case. The heating of the sample could be done by passing current through a 0.05 mm Ta strip, uniformly pressed between the sample and the case. The STO crystal temperature was measured with a NiCr–NiAl thermocouple spot welded onto the case. The thermocouple was calibrated by an infrared pyrometer in the 250–1100 °C temperature range. The cleaning process of the sample was achieved by Ar^+ ion sputtering with energy 2 keV, at argon gas pressure $\sim 10^{-6}$ Torr, for ~30 min bombarding time. The restoration of the 1×1 symmetry of the substrate was achieved through annealing at about 400 °C after the ion bombardment.

The TDS experiments were carried out with a linear rate of the sample heating of ~ 17 K s^{-1}. The experimental error of desorption temperatures was estimated at about ±20 K. The AES measurements were performed by utilizing a primary electron beam with energy 2 keV. The AES as well as EELS spectra were recorded by the CMA in the first derivative mode, $dN(E)/dE$, and the signal intensity was measured from the peak to peak height (AP-PH). The changes of the WF of the surface were recorded by measuring the characteristic *I*–*V* curve of a diode, formed with an electron gun playing the role of the cathode and the substrate that of the anode. The accuracy of the relative WF measurements was about ±0.05 eV.

Finally, cesium was deposited on the substrate by evaporation from a commercial SAES Getters source. The heating current of the source during the evaporation was constant at 6.0 A. The coverage of the surface was measured in monolayers (MLs), where 1 ML of Cs on the STO(100) surface was defined equal to 6.56×10^{14} atoms cm^{-2}. This figure was derived from the lattice constant 3.905 Å of the square unit cell of the TiO_2 terminated STO(100) surface.

3. Results and discussion

We deposited cesium on the clean STO(100) surface at RT in steps of 2 min deposition time. Figure 1 shows the AP-PH of Cs (47 eV), O (510 eV) and Ti (380 eV) as a function of Cs deposition time on the STO(100) surface at RT. The intensity of the Cs (47 eV) Auger electron transition line (AETL) increases linearly with Cs deposition time up to about 16 min, while the substrate signals O (510 eV) and Ti (380 eV) decrease linearly. After that time the Cs (47 eV) AP-PH increases very slowly, while the substrate signals remain almost constant. In general, the linear variation of the AP-PH of the adsorbate and the substrate AETLs versus deposition time, is characteristic of a layer by layer growth (FM mode) [20]. The appearance of breaks in the growth curves, are commonly assigned to the completion of successive layers. Here in figure 1, we observe only a single break at ~16 min for each AETLs growth curve, while the variation of all the AES signals is almost negligible for deposition time >16 min. From these AES measurements, we conclude that Cs on the STO(100) surface at RT develops in a single layer with constant sticking coefficient up to the deposition of ~16 min. Above this adsorbed quantity, the sticking coefficient of Cs decreases drastically, preventing the development of a second Cs layer. This behavior is characteristic of Cs deposition on metallic surfaces [21, 22] as well as on the silicon surface [23], where only a single layer of Cs grows on the surface at RT. In contrast, this Cs growth is different to that on the layer compound MoS_2 [24, 25], where the variation of the AP-PHs of both the adsorbate and the substrate are not

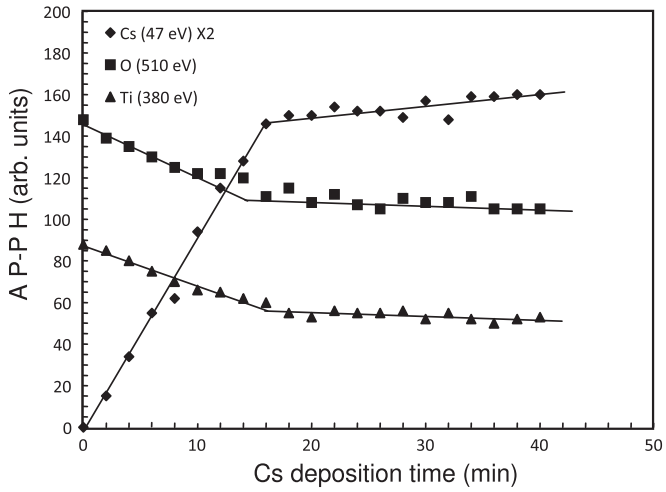

Figure 1. The intensity (AP-PH) of the Cs (47 eV), O (510 eV) and Ti (380 eV) Auger electron transition lines as a function of the Cs deposition time on the STO(100) surface.

linear indicating the formation of three-dimensional (3D) clusters or 3D islands on the insulating surface of NiO [26]. The behavior of the Cs (563 eV) AETL is almost the same with that of Cs (47 eV) and is not shown here. The cesium overlayer should be amorphous, since the 1 × 1 LEED pattern of the clean STO(100) surface gradually disappeared. No order was observed with Cs deposition up to 40 min. Furthermore, the annealing of the cesiated surface in steps of 100 K up to 900 K, apart from the reappearance of the 1 × 1 substrate symmetry, did not show any new ordering. The reappearance of the STO 1 × 1 symmetry is attributed to the uncovering of the substrate, due to the gradual desorption of Cs at high temperature. Here we need to note, that the small increase of the Cs (47 eV) AP-PH recorded after 16 min, is probably due to an additional Cs deposition on the oxygen contaminated cesiated STO surface. Indeed, due to the high reactivity of the Cs overlayer to oxygen [21] and the long time of adsorption experiments, it is likely that oxygen atoms coming from the environment, stick onto the cesiated surface and act as nucleation centers for some extra cesium adsorption. Actually, Papageorgopoulos has shown that the maximum adsorbed Cs quantity on MoS_2 at RT, can be increased by alternate adsorption of Cs and O_2, provided someone starts with Cs deposition [24]. We believe, however, that this effect should be of minor extent, since the increase of the Cs(47 eV) AP-PH after 16 min is very weak.

From the attenuation of the Ti(380 eV) AETL, we can calculate the average thickness of the Cs overlayer. Based on the equation

$$I = I_o e^{-d/\lambda \cos\theta}, \tag{1}$$

where I and I_o is the AP-PH signal of the Ti(380 eV) AETL from the cesiated and the clean STO(100) surface respectively, d is the average layer thickness, λ is the electron attenuation length, and $\theta = 42^\circ$ is the effective mean acceptance angle of the CMA. It is known that the measured electron attenuation length depends on inelastic as well as on elastic electron scattering. The ratio between the electron attenuation length λ and the inelastic mean free path (IMFP) is given by the following equation [27],

$$\frac{\lambda}{\lambda_{\mathrm{IMFP}}} = \left(1-0.028\sqrt{Z}\right)(0.501+0.068 \ln E), \tag{2}$$

where λ_{IMFP} is the IMFP, Z is the atomic number of the overlayer and E is the kinetic energy of the substrate Auger electrons.The λ_{IMFP} of the emitted Ti(380 eV) Auger electron traveling through the cesium overlayer, is calculated from the Bethe equation [28],

$$\lambda_{\mathrm{IMFP}} = E/\left[E_p^2 \beta ln(\gamma E)\right], \tag{3}$$

where E is the kinetic energy of the emitted Ti Auger electron, E_p is the free-electron plasmon energy of cesium (in eV), while β and γ are constants depending on the atomic properties of cesium. Both of these constants are given from the following empirical equations [28],

$$\beta = -0.0252+1.05\left(E_p^2 - E_g^2\right)^{-1/2} + 8.10\times10^{-4}\rho \tag{4}$$

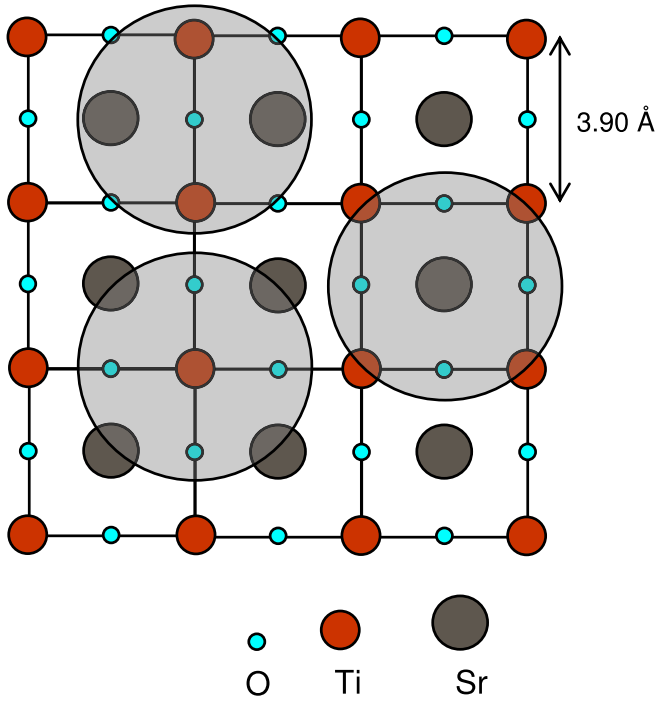

Figure 2. Simplified adsorption model of Cs on the TiO_2 terminated STO(100) surface. Three different top adsorption sites on Sr, Ti and O atoms are considered. The Cs adatoms are drawn with big transparent grey cycles proportional to the atomic size.

and

$$\gamma = 0.151\rho^{-1/2}, \tag{5}$$

where ρ is the density of cesium (in g cm^{-3}) and E_g is the energy gap of the material, which is zero for cesium. By using an experimental value of the bulk electron plasmon of Cs equal to $E_p = 4.6$ eV, measured for a Cs ML on Mo(110) [22], and inserting the cesium density equal to 1.9 g cm^{-3} in equations (4) and (5), equation (3) results in a λ_{IMFP} equal to 23.6 Å. Then from equation (2) we calculate the electron attenuation length λ equal to 16.9 Å. Finally, from equation (1) we calculate the average Cs layer thickness, $d = 5.00$ Å. This value approximates the atomic diameter of Cs, $d_{Cs} = 5.31$ Å, indicating that the full amorphous physical layer of Cs on the STO(100) surface formed after 16 min of deposition, is rather uniform with about one atom thickness.

Although the absence of a symmetrical overstructure of Cs on STO, makes the exact determination of coverage difficult, taking into account that the calculated thickness of the Cs overlayer is near to the atomic size of cesium, we estimated the coverage by performing adsorption simulations, by using a 12 × 12 lattice of a TiO_2 terminated STO(100) surface with lattice constant equal to 3.90 Å. The edge atoms were constrained to the following periodic boundary conditions: atoms of the 12th line neighbor atoms of the first line, and atoms of the 12th column neighbor atoms of the first column. The Cs adatoms which were considered to have the atomic diameter of bulk Cs, were immobile and randomly adsorbed at three different top adsorption sites as figure 2 depicts. Towards the completion of the single layer, however, we allowed the relaxation of Cs adatoms even at some different non top adsorption sites, in order to end up with a more complete and homogeneous layer. By using an algorithm for selecting randomly the adsorption sites, and after 5 runs, the coverage of the complete Cs layer on STO(100) was calculated equal to 0.45 ± 0.01 ML. If we consider a constant sticking coefficient of Cs on the surface, a deposition rate of ~0.028 ML min^{-1} is estimated.

Figure 3 shows the WF change $\Delta\Phi$ versus Cs deposition time on the STO(100) surface at RT. The WF of the STO initially decreases rapidly, whereas as the deposition time increases, the WF decreases more slowly. At about 9 min (~0.25 ML), the curve passes through a minimum at $\Delta\Phi = -2$ eV, and then increases slightly to a maximum value forming a plateau, which corresponds to a WF ~1.86 eV lower than that of the clean STO surface. For coverages higher than 12 min (0.34 ML), the WF remains constant. The above described WF variation is typical of that of the layer growth mode of Cs on metallic substrates [21, 29, 30], and more generally similar to that of alkali metal adsorption on metals and silicon surfaces [31]. Taking into account the WF of the clean STO surface 4.1 eV [32, 33], we calculate the WF of the surface at higher Cs coverage (⩾0.34 ML) equal to ~2.24 eV. This value is close to 2.14 eV, the WF of the metallic polycrystalline Cs [34, 35]. The initial slope of the $\Delta\Phi$ versus time curve is proportional to the dipole moment of the initially isolated Cs adatoms, as described by the Helmholtz equation [36, 37]. Therefore, the large slope of the WF curve at very low coverage indicates that

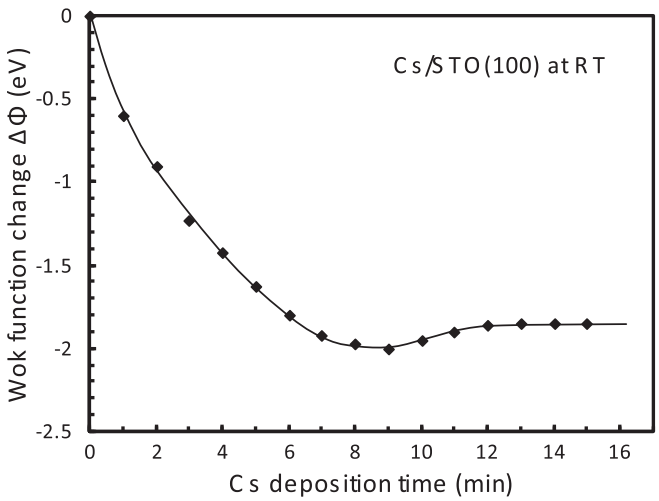

Figure 3. The work function change $\Delta\Phi$ of the Cs/STO(100) surface as a function of the Cs deposition time.

initially cesium is adsorbed in the form of ions or strongly polarized atoms [38]. As the Cs coverage increases, the slope of the WF curve decreases due to depolarization effects among the adatoms, passes through a minimum and finally levels off to a maximum value. The increase of the WF above 0.25 ML is attributed to a Cs–Cs interaction setting in, while the plateau formation indicates the metallization of the Cs overlayer [23, 39]. Combining the above WF results, with the previously described AES measurements, we conclude that Cs on the STO(100) surface at RT, forms a single rather metallic layer. Although this mode of deposition happens on metallic substrates, it does not occur on oxides such as NiO [26] or on layered compounds such as MoS_2 [25].

Figure 4 shows the EELS spectra of the STO (100) surface after Cs deposition, taken with primary electron energy of 100 eV. The clean STO surface shows the characteristic loss peaks at 9.1, 12.7, 22.7, 28.6 and 36.8 eV. The allocated loss peaks are defined at the local maximum slopes in the EELS curves, denoted by the dashed vertical lines. According to previous results, the intense 9.1 and 12.7 eV peaks are attributed to interband transitions of the valence electrons of O 2p to the unoccupied Ti 3d states within the conduction band [40–42]. The peak at 28.6 eV is attributed to the bulk plasmon of STO [41, 43, 44], whereas the peak at 22.7 eV approaches the energy of the expected surface plasmon [44, 45]. Another, however, possible origin of the latter loss could be the ionization of the Sr 4d doublet. Finally, the 36.8 eV peak is probably related to transitions of the Sr 4s or Ti 3p electrons to final states in the conduction band or to localized excited states [43].

As the Cs deposition time increases, both of the loss peaks at 12.7 and 9.1 eV gradually diminish. The loss at 12.7 eV seems to vanish and a new loss at ~15 eV appears at ~2 min, while that at 9.1 eV decreases rapidly. The latter loss, however, strengthens again for depositions above 9 min. Perhaps this happens due to residual oxygen from the surroundings as we mentioned before. Another change in EELS spectra is the quite early disappearance of the loss at ~22.7 eV at about 0.5 min, which strengthens the assertion of this peak as a surface plasmon peak. Instead, the gradual development of loss at the energy ~19.3 eV is observed, while the bulk plasmon loss remains even at higher coverages. The new losses at ~15 and 19.3 eV are attributed to the cesium overlayer. In fact, Kiskinova *et al* [46] have recorded a double loss at 14.2 and 12.2 eV, which has been attributed to the Cs 5p electrons excitations. In addition, within the same energy region, Francioni *et al* [47] have measured a shallow 5p core levels doublet in the valence band of a cesium ML on the Si(111) surface. Accordingly, this doublet could be identified with the recorded 15 eV loss, which probably due to the limited resolution appears to be a single loss feature. The origin of the 19.3 eV loss is rather uncertain. A possible explanation could be the Sr 4p excitations into a Cs resonance level (at low coverages) or into the Cs conduction band (at high coverages). A similar explanation has been given for the adsorption of Cs on the GaAs(100) surface, where unresolved losses at 20–23 eV were attributed to Ga 3d excitations into Cs resonance levels or the conduction band [48].

Figure 5 shows the thermal desorption spectra of Cs after deposition of different amounts of cesium on the clean STO(100) surface. At low coverages (<5 min or 0.14 ML) the Cs QMS signal consists of two thermal desorption peaks (TD peaks) denoted as β_1 and β_2 at ~960 K and ~1200 K respectively. As the coverage increases, the β_2 peak develops at the same temperature up to 7 min, whereas for longer depositions it appears at slightly higher temperature ~1240 K. The β_1 TD peak develops in parallel to the β_2 one. For deposition time $\geqslant$5 min, a third β_3 TD peak appears, which moves to lower temperature as the coverage increases. The β_3 TD peak stabilizes at ~490 K for coverage $\geqslant$10 min, while the cesium desorption related to that peak starts just above the RT. The three main TD peaks grow simultaneously and almost saturate after deposition at about

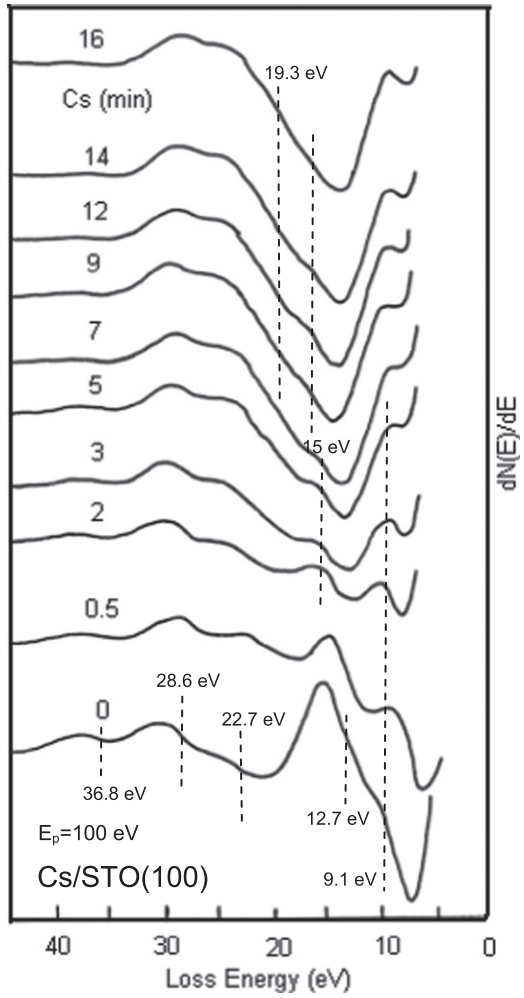

Figure 4. The EELS spectra for Cs adsorption on the STO(100) surface at RT at different coverages.

20 min. For deposition above 10 min, however, a fourth TD peak β_4 appears at ~840 K with a weak shoulder at ~740 K. This new TD peak is adjacent to the β_1 and strongly overlaps with it. The simultaneous growth of the three TD peaks at about 840, 970 and 1200 K respectively, probably indicates that in the submonolayer regime, there are three different adsorption energy states of Cs adatoms on the STO(100) surface. It is tempting to associate these three adsorption states with the three different adsorption sites as depicted in figure 2, for modeling the Cs adsorption. However, theoretical binding energy calculations are needed to reveal the correlation between the recorded TD peaks and the proposed adsorption sites. The first appearing β_1 peak grows in parallel with the β_2 one for coverage up to ~5 min. The appearance of the lower temperature β_3 peak at coverage of ~7 min, almost coincides with the WF minimum (figure 3), suggesting probably the beginning of the interaction between Cs adatoms. Moreover, the β_3 peak maximization corresponds to the stabilization of the WF of the surface, becoming nearly equal to that of the metallic Cs. Therefore it is reasonable to attribute the origin of the β_3 desorption peak to Cs in the metallic state. This argument is supported by the fact that for deposition time $\geqslant$10 min (0.28 ML), the desorption of Cs starts just above 300 K, close to the sublimation temperature of Cs [49]. As the coverage approaches the full Cs layer, a fourth desorption phase β_4 starts to occur too.

Assuming that the desorption of Cs is a first order desorption, we calculate the desorption activation energy E of cesium atoms by the following equation given by Readhead [50]

$$E = RT\left[\ln\left(\frac{\nu T}{\kappa}\right) - 3.64\right], \tag{6}$$

where $R = 5.189 \times 10^{19}$ eV mol^{-1} K^{-1} is the gas constant, T is the desorption temperature, ν is a frequency factor ~10^{13} s^{-1}, and κ is the heating rate of the sample ~17 K s^{-1}. Using equation (6), we finally report in table 1 the desorption activation energies of all the recorded TD peaks.

Generally speaking, the broad line-shape of the TDS spectra in figure 5, supports the formation of a uniform layer of Cs on the surface, in line with previous results of Cs on metallic [30] and semiconducting surfaces

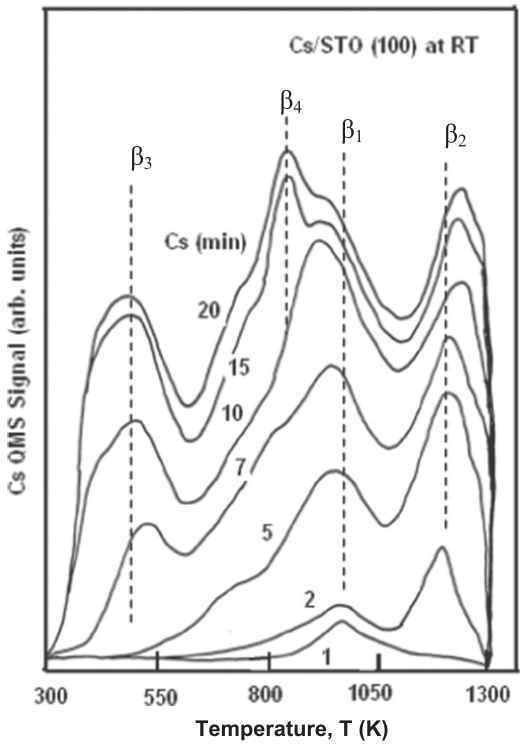

Figure 5. The TDS spectra for Cs adsorption on the STO(100) surface at RT at different coverages.

Table 1. The calculated desorption activation energies of Cs on the STO(100) surface. The uncertainty in the TD peak temperature (∼ ±20 K), results in an uncertainty of the desorption activation energy.

TD peak	Temperature (K)	Desorption energy (eV atom^{-1})
β_1	970	2.18 (±0.05 eV)
β_2	1200	3.16 (±0.05 eV)
β_3	490	1.25 (±0.05 eV)
β_4	840	2.18 (±0.05 eV)

[23, 48]. This behavior is very different from that of Cs on NiO [26] and MoS_2 [25], where the TD spectra are narrow and the desorption process initiates above 600 K even at high coverage. The simultaneous growth of the two high temperature desorption peaks, β_1 at ∼970 K and β_2 at ∼1200 K, appears from very low Cs coverage. This result is different to that of Cs on the metallic substrate of W(110), where the high temperature TD peak firstly saturates at low coverage, whereas at higher Cs coverage desorption occurs at much lower temperature [30]. This probably means that the Cs atoms on the W(110) surface, firstly occupy high energy adsorption states, while after the saturation of these states the Cs atoms adsorb in lower energy adsorption states. On the other hand, the Cs atoms on the STO(100) surface, occupy two different adsorption states simultaneously, whereas above 10 min (0.28 ML), the metallization of the overlayer starts. This suggests that Cs adsorption on the STO (100) surface shows a mixed behavior compared to that of Cs on metallic and on insulating surfaces. Desorption of the cesium overlayer, does not only give the β_3 peak but also those at higher energies β_1, β_2, and β_4 TD peaks. This indicates that only a part of the metallic Cs is desorbing, while the rest diffuses across the surface to more strongly bound energy states, related to the β_1, β_2 and β_4 TD peaks.

The area under the Cs TDS spectra as a function of deposition time is shown in figure 6(a). The TDS area is analogous to the desorbing amount of Cs on the surface and thus is proportional to the coverage. We observe a linear increase of the Cs TDS area versus the deposition time, which suggests a constant sticking coefficient of Cs on STO(100). This is in accordance to the calibration of coverage from the AES measurements. The Cs TDS area slightly increases for coverages >16 min (0.45 ML), consistent with the Cs (47 eV) AP-PH variation. In conclusion, the comparison of figure 6(a) with the Cs AES growth line (figure 1), suggests that Cs at RT forms a single layer on STO surface as on metallic substrates.

Figure 6(b) shows the AP-PH of Cs (47 eV) AETL after Cs deposition of 16 min (0.45 ML) at RT, and subsequent annealing to higher temperatures for annealing time ∼1 min at each temperature. The AES spectra

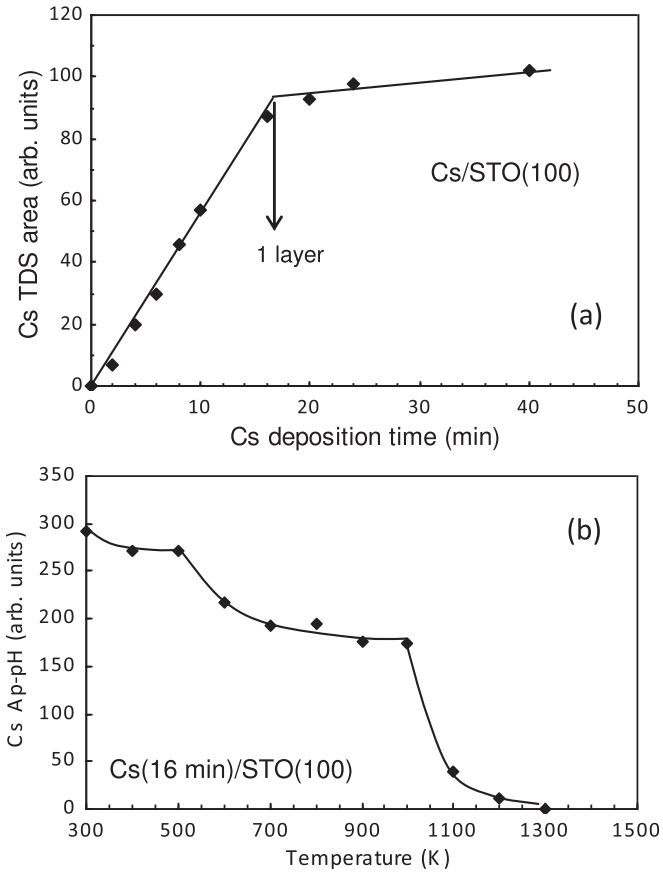

Figure 6. (a) The area of the Cs TDS spectra as a function of the deposition time for Cs adsorption on the STO(100) surface at RT. The physical layer coverage 0.45 ML is estimated at ∼16 min deposition time. (b) The Cs (47 eV) AP-PH as a function of the annealing temperature of the full layer of Cs on the STO(100) surface.

were received with the sample near to RT. It is observed that the Cs AES signal decreases rapidly with increasing temperature and shows three main desorption states at about 300–400 K, 500–800 K and 1000–1200 K. The above described AP-PH signal reduction versus the annealing temperature, is consistent with the cesium desorption states described in TDS spectra (figure 5). It is noteworthy that the Cs signal reduced down to zero for substrate annealing up to 1300 K. This is an indication that no Cs diffusion into the bulk takes place during the desorption process. In contrast, Cs showed a diffusion into the bulk of MoS_2, where complete desorption from the surface could not be realized by annealing [24].

We also measured the O(510 eV)/Ti(380 eV) AP-PH ratio (not shown) first as a function of Cs deposition at RT, and second after subsequent annealing in steps of 100 K up to 1300 K. Those two AETLs have almost the same escape depth and their ratio is a good index of possible reordering of the surface Ti and O atoms. In all the cases, the ratio was found almost constant, implying that no reordering or chemical composition change of the Cs/STO interface takes place. This may indicate that the Cs overlayer does not interact strongly with the surface by forming chemical compounds. An additional indication to that, is the absence of desorbing Cs_2O compound in the QMS spectra. However, it could be claimed that annealing of the substrate possibly dissociates some Cs–O compounds formed at RT. Nevertheless, the oxidation of the Cs overlayer by a reduction process of the STO surface at RT, should have given much lower final WF since, depending on the thickness, Cs_2O presents an ultimate low WF of ∼0.7 eV [51]. This further supports that the STO surface remains rather inert and stable during Cs adsorption. More direct evidence such as XPS measurements [52], however, is needed to verify that no interfacial chemical reaction takes place across the Cs/STO(100) interface at RT.

Regarding the chemical stability of the MO interface, Fu and Wagner have shown that the occurrence of interfacial chemical reactions, depend to a great extent on the Fermi levels of the contacting phases of the two materials [52, 53]. According to their model, if $E_F(M) > E_F(MO)$, where E_F(M and E_F(MO) are the Fermi levels of the metal adsorbate (M) and the MO substrate respectively, the alignment of E_F at the interface, induces charge transfer from the metal to the oxide substrate adsorbate. This charge transfer builds an electric field at the interface, pointing from the metal to the bulk oxide, enhancing the oxygen anion diffusion towards the interface and favouring the onset of interfacial interactions. In our case considering the WF of the Cs overlayer ∼2.24 eV,

and that of STO equal to ~4.1 eV, the relationship $E_F(M) > E_F(MO)$ holds, and thus a Cs–O interaction is in principle favoured. However, we have no indication for chemical compounds formation between O and Cs adatoms. This might be due to the fact that apart from the charge transfer, thermodynamic and kinetic criteria are also playing important role in the substrate reduction. Indeed, previous works concerning Li [16], K [17], Fe [54], Ni [55] and Ba [56] adsorption on the STO(100) surface, supports that the interfacial oxidation of the adsorbate is a complex process depending on a combination of charge transfer, thermodynamic and kinetic phenomena at surface.

Studying the Cs–STO interface from the thermodynamic point a view, Cs reduces the TiO_2 terminated STO (100) surface according to the equation

$$2Cs(s)+TiO_2(s) \rightarrow TiO(s)+Cs_2O(s),$$

where (s) refers to the solid phase, since the equation describes a solid–solid chemical reaction. In general, a reaction like that is thermodynamically downhill if the overall enthalpy change is negative. Considering the enthalpies of formation of TiO_2 equal to -944 kJ mole^{-1}, of TiO, -520 kJ mole^{-1}, and that of Cs_2O, -346 kJ mole^{-1} [57], we conclude that the reduction of the STO by Cs is not thermodynamically favoured. This might be a reason for not detecting a C_2O compound. Another surface reaction that someone should consider is the following:

$$2Cs(s)+2TiO_2(s) \rightarrow Cs_2O(s)+Ti_2O_3(s),$$

where Cs reduces the substrate into the lower oxide Ti_2O_3 , with enthalpy formation of -1521 kJ mole^{-1} [52]. Again, based on the enthalpy change, the reaction is marginally not energetically favorable. Another reason for not observing cesium oxidation might be kinetic limitations. Apparently, in addition to the activation barrier for desorption, there should be an activation barrier for surface reaction. The absence of the Cs–O compound, suggests that the activation energy for desorption is probably lower than that of the reaction.

Finally, it is interesting to compare the Cs adsorption on the STO(100) surface with that of other alkalis such as Li and K, studied by Mori and Kamaratos [16, 17]. In the case of K, two-dimensional (2D) islands grow on the surface [17]. Despite the evidence of interaction among the K adatoms, no clear indications of the adsorbate metallization were reported. Instead, a charge transfer from K 4s to the substrate Ti 3d states was measured, while no K–O compounds were detected. In the case of Li adsorption on STO [16], again no metallization of the adsorbate was reported, but instead a Li–O intermixing was documented. Since no charge transfer was measured between Li and STO, a covalent instead of an ionic bonding was proposed for the Li adatoms. Furthermore, there are indications for partial Li intercalation into the substrate. Comparing the cesium behavior to that of potassium and lithium, we point out a difference, since a single rather metallic layer is formed instead of islands, or surface intermixing. The larger atomic size compared to those of the two other alkalis, in combination with the relatively weak interaction between Cs–STO, probably enhance the Cs–Cs interaction, leading the overlayer into the metallic phase. In contrast, Li due to its small atomic size, intermixes and/or intercalates into the substrate, hindering the interaction between the adatoms, and thus preventing the metallization. Potassium, on the other hand, is of comparable atomic size with cesium. However, no clear indications for the metallization of K are given [17]. It is possible that the observed charge transfer from K 4s to Ti 3d states and the kinetics growth in 2D islands may prevent the potassium metallization.

4. Conclusions

The growth of Cs on the STO(100) surface at RT was investigated by means of AES, LEED, EELS, TDS and relative WF measurements. The results show that at low coverages the Cs adatoms are isolated and strongly bound to the surface, while as the coverage increases, the adatoms start to interact with each other, forming finally a 2D amorphous metallic overlayer. The sticking coefficient of cesium deposition remains constant. There are no indications for Cs–O compounds formation. Thermal annealing of the substrate causes a partial desorption of the metallic overlayer, while at the same time surface diffusion of the remaining Cs atoms takes place into more strongly bound adsorption states. The behavior of Cs on STO differs from that of other alkalis such as lithium and potassium, in terms of growth and desorption properties.

References

[1] Rühle M, Evans A G, Ashby M F and Hirth J P (eds) 1990 *Metal–Ceramic Interfaces* (Oxford: Pergamon)
[2] Ernst F 1995 *Mater. Sci. Eng. Rep.* **14** 97
[3] Fu Q and Wagner T 2007 *Surf. Sci. Rep.* **62** 431
[4] Cambell C T 1997 *Surf. Sci. Rep.* **27** 1
[5] Henry C R 1998 *Surf. Sci. Rep.* **31** 235
[6] Linsebigler A L and Yates J T 1995 *Chem. Rev.* **95** 735
[7] Pennicott K 2001 *Phys. World* **14** 6

[8] Wagner S F, Warnke C, Menesklou W, Argirusis C, Damjanović T, Borchardt G and Ivers-Tiffée E 2006 *Solid State Ion.* **177** 1607
[9] De Teresa J M, Barthélémy A, Fert A, Contour J P, Montaigne F and Seneor P 1999 *Science* **286** 507
[10] Kittl J A *et al* 2009 *Microelectron. Eng.* **86** 1789
[11] Wang L-Q, Ferris K F, Azad S and Engelhard M H 2005 *J. Phys. Chem.* B **109** 4507
[12] Li W, Liu S, Wang S, Guo Q and Guo J 2014 *J. Phys. Chem.* C **118** 2469
[13] Mavroides J G, Kafalas J A and Kolesar D F 1976 *Appl. Phys. Lett.* **28** 241
[14] Wrighton M S, Ellis A B, Wolczanski P T, Morse D L, Abrahamson H B and Ginley D S 1976 *J. Am. Chem. Soc.* **98** 2774
[15] Yin J, Ye J and Zou Z 2004 *Appl. Phys. Lett.* **85** 689
[16] Mori E E and Kamaratos M 2007 *J. Phys.: Condens. Matter* **19** 356001
[17] Mori E E and Kamaratos M 2006 *Surf. Rev. Lett.* **13** 681
[18] Lopez A, Heller T, Bitzer T, Chen Q and Richardson N V 2001 *Surf. Sci.* **494** L811
[19] Wang J, Li Z and Zou Z 2013 *Appl. Surf. Sci.* **270** 359
[20] Argile C and Rhead G E 1989 *Surf. Sci. Rep.* **10** 277
[21] Papageorgopoulos C A 1982 *Phys. Rev.* B **25** 3740
[22] Gorodetsky D A, Melnik Y P, Usenko V A, Yas'ko A A and Yarigin V I 1994 *Surf. Sci.* **315** 51
[23] Kennou S, Kamaratos M, Ladas S and Papageorgopoulos C A 1989 *Surf. Sci.* **216** 462
[24] Papageorgopoulos C A 1978 *Surf. Sci.* **75** 17
[25] Kennou S, Ladas S and Papageorgopoulos C 1985 *Surf. Sci.* **152/153** 1213
[26] Kennou S, Kamaratos M and Papageorgopoulos C A 1991 *Surf. Sci.* **256** 312
[27] Briggs D and Seah M P 1990 *Practical Surface Analysis* 2nd edn vol 1 (Chichester: Wiley)
[28] Tanuma S, Powell C J and Penn D R 1988 *Surf. Interface Anal.* **11** 577
[29] Papageorgopoulos C A and Chen J M 1975 *Surf. Sci.* **52** 40
[30] Desplat J L and Papageorgopoulos C A 1980 *Surf. Sci.* **92** 97
[31] Bonzel H P, Bradshaw A M and Ertl G 1989 Physics and chemistry of alkali metal adsorption *Materials Science Monographs* vol 57 (Amsterdam: Elsevier)
[32] Chung Y-W and Weissbard W B 1979 *Phys. Rev.* B **20** 3456
[33] Zagonel L F, Bäurer M, Bailly A, Renault O, Hoffmann M, Shih S-J, Cockayne D and Barrett N 2009 *J. Phys.: Condens. Matter* **21** 314013
[34] Boutry G A and Dormont H 1969 *Philips Tech. Rev.* **30** 225
[35] Michaelson H B 1977 *J. Appl. Phys.* **48** 4729
[36] Langmuir I 1932 *J. Am. Chem. Soc.* **54** 2798
[37] Hölzl J, Schulte F K and Wagner H , 1979 Solid Surface Physics *Springer Tracts in Modern Physics* vol 85 (Berlin: Springer)
[38] Wimmer E, Freeman A J, Hiskes J R and Karo A M 1983 *Phys. Rev.* B **28** 3074
[39] Fedorus A G and Naumovets A G 1970 *Surf. Sci.* **21** 426
[40] Henrich V E, Dresselhaus G and Zeiger H J 1978 *Phys. Rev.* B **17** 4908
[41] Kohiki S, Arai M, Yoshikawa H, Fukushima S, Oku M and Waseda Y 2000 *Phys. Rev.* B **62** 7964
[42] Van Benthem K, French R H, Sigle W, Elsässer C and Rühle M 2001 *Ultramicroscopy* **86** 303
[43] Bermudez V M and Ritz V H 1980 *Chem. Phys. Lett.* **73** 160
[44] Andersen J E T and Møller P J 1990 *Thin Solid Films* **186** 137
[45] Vlachos D, Kamaratos M, Foulias S D, Argirusis C and Borchardt G 2004 *Surf. Sci.* **550** 213
[46] Kiskinova M, Tikhov M and Surnev L 1990 *Surf. Sci.* **238** 25
[47] Franciosi A, Soukiassian P, Philip P, Chang S, Wall A, Raisanen A and Troullier N 1987 *Phys. Rev.* B **35** 910
[48] Kamaratos M and Bauer E 1991 *J. Appl. Phys.* **70** 7564
[49] Lide D R (editor in chief) 1998–1999 *CRC Handbook of Chemistry and Physics* 79th edn (Boca Raton, FL: CRC Press)
Kittel Ch. 2005 *Introduction the Solid State Physics* 8th edn (New York: Wiley)
[50] Redhead P A 1962 *Vacuum* **12** 203
[51] Uebbing J J and James L W 1970 *J. Appl. Phys.* **41** 4505
[52] Fu Q and Wagner T 2005 *J. Phys. Chem.* B **109** 11697
[53] Fu Q and Wagner T 2005 *Surf. Sci. Lett.* **574** L29
[54] Kamaratos M, Vlachos D and Foulias S D 2008 *J. Phys.: Condens. Matter* **20** 315009
[55] Vlachos D, Kamaratos M, Foulias S D, Argirusis C and Borchardt G 2004 *Surf. Sci.* **550** 213
[56] Vlachos D, Kamaratos M, Argirusis C and Foulias S D 2012 *J. Electron Spectrosc. Relat. Phenom.* **185** 615
[57] Lide D R (ed) 1998 *CRC Handbook of Chemistry and Physics* (Boston, MA: CRC Press)